Selenomethionine mitigate PM2.5-induced senescence of alveolar epithelial cells via attenuating inflammatory response mediated by cGAS/STING/NF-κB pathway

Xiaofei Wang
Hefei University
Xuanyi Xia
Hefei University
Wenzun Lu
Hefei University
Yuchen Zhu
Hefei University
Chunmei Ge
Hefei University
Xiaoying Guo
Anhui Academy of Agricultural Science
Ning Zhang
Hefei University
Hua Chen
Hefei University
Shengmin Xu (shmxu@mail.ustc.edu.cn)
Anhui University

Research Article

Keywords: Particulate matter 2.5 (PM2.5), Inflammation, Senescence, Selenium, Cyclic guanosine monophosphate (GMP)-adenosine monophosphate (AMP) synthase (cGAS)

Posted Date: April 13th, 2022

DOI: https://doi.org/10.21203/rs.3.rs-1532157/v1

Abstract

Particulate matter 2.5 ($PM_{2.5}$) is a widely known atmospheric pollutant which could induce the aging-related pulmonary diseases such as acute respiratory distress syndrome (ARDS), chronic obstructive pulmonary disease (COPD) and interstitial pulmonary fibrosis (IPF). In recent years, with the increasing atmospheric pollution, airborne fine $PM_{2.5}$, which is an integral part of air pollutants, has become a thorny problem. Hence, this study focused on the effect of $PM_{2.5}$ on the senescence of pulmonary epithelial (A549) cells, identifying which inflammatory pathway mediated $PM_{2.5}$-induced cellular senescence and how to play a protective role against this issue. Our data suggested that $PM_{2.5}$ induced time- and concentration-dependent increasement in the senescence of pulmonary epithelial cells. Using a inhibitor of cGAS (PF-06928215) and a inhibitor of NF-κB (BAY 11-7082), it was revealed that $PM_{2.5}$-induced senescence was regulated by inflammatory response, which was closely related to the cGAS/STING/NF-κB pathway activated by DNA damage. Moreover, our study also showed that when A549 cells were exposed to 100 μg/mL $PM_{2.5}$ for 48 h, the pretreatment with 20 μM selenomethionine (Se-Met) for 12 h could inhibit inflammatory response and prevent cellular senescence by hindering cGAS/STING/NF-κB pathway. These findings indicated that selenium made a defense capability for $PM_{2.5}$-induced senescence of alveolar epithelial cells, which provided a novel insight for resisting the harm of $PM_{2.5}$ to human health.

Introduction

Since the smog episode in London in the middle of last century, the problem of air pollution has attracted more and more attention. Nowadays, with the increasing pollution, airborne fine particulate matter 2.5 ($PM_{2.5}$), which is an integral part of air pollution, has become a public health problem of widespread concern. $PM_{2.5}$ is defined as the fine particles with diameter ≤ 2.5 μm in total suspended particles in the atmosphere, which will be harmful to the respiratory system, central nervous system, circulatory system and other human systems [1, 2]. Among them, the respiratory system as the main route of $PM_{2.5}$ to enter the human body was particularly affected. The lung, as an important organ of the respiratory system, was in direct contact with $PM_{2.5}$ in the air. Studies have shown that $PM_{2.5}$ can lead to a variety of toxic effects in the lung, such as inflammatory response, oxidative stress, immunotoxicity and genetic damage [3]. Moreover, inflammatory response and genetic damage were demonstrated to be closely related to the senescence of lung organ [4, 5]. Additionally, the senescence of lung organ will further aggravate the development of respiratory diseases [6]. Recent studies have suggested that respiratory diseases such as acute respiratory distress syndrome (ARDS), chronic obstructive pulmonary disease (COPD) and interstitial pulmonary fibrosis (IPF) are all correlated with $PM_{2.5}$ exposure [7, 8].

Senescence was a phenomenon that mammalian cells lost their ability of replication and entered a permanent stagnation state of growth cycle [9]. It was demonstrated to be closely related to the aging of the organism. When senescent cells were escaped from clearance by immune system in time, they accumulated and secreted various cytokines into the tissue, which changed the microenvironment of the

tissue, affected the differentiation and growth of the surrounding cells, and eventually led to the deterioration of tissue and organ [10]. Additionally, it was suggested that there was a close relationship between inflammation and senescence. Han et al. found that IL-1β overexpression could activate IL-1β/NF-κB/p53/p21 pathway in vascular smooth muscle cells (VSMCs), and then lead to premature cellular senescence with upregulated senescence-associated β-galactosidase (SA-β-gal) activity [11]. Gao et al. also found that bleomycin could induce increased expression level of inflammatory cytokines such as IL-1β, IL-6, TNF-α and activate SA-β-gal, and therefore induce the senescence of annulus fibrosus-derived stem cells (AFSCs) in rabbit. Meanwhile, with joint treatment with rapamycin and bleomycin, the expression of inflammatory cytokines in AFSCs was inhibited, which delayed cellular senescence [12]. In addition, Tichy et al. have shown that abnormal activation of NF-κB for a long time can lead to shortened telomeres and Ku80 dysregulation of muscle stem cells (MuSCs) [13].

Cyclic guanosine monophosphate (GMP)-adenosine monophosphate (AMP) synthase (cGAS) was an important component of the natural immune system, which could recognize exogenous DNA in the cytoplasm from viruses, bacteria and protozoa, and induced the generation of cyclic GMP-AMP (cGAMP) [14]. By activating stimulator of interferon gene (STING) and nuclear factor kappa-B (NF-κB), cGAMP promoted the secretion of inflammatory cytokines such as TNF-α, IL-6 and IL-8, which led to senescence-associated secretory phenotype (SASP) and induced cellular senescence [15]. However, recent studies have found that the cGAS/STING pathway could not only recognize the exogenous DNA in the cytoplasm, but also perceive the endogenous DNA due to DNA double-strand breaks and other ways, which might play a major role in the occurrence of senescence [16]. For instance, Bi et al. found that mitochondrial damage resulting from oxidative stress primed the cGAS/STING pathway to trigger IFN-I response in vascular smooth muscle cells (VSMCs), and subsequently promoted VSMCs premature senescence, resulting in chronic kidney disease (CKD)-associated plaque vulnerability [17]. Kwon et al. also found that the inhibition of serum/glucocorticoid related kinase 1 (SGK1) as the stimulator of DNA damage prevented glial cell senescence by suppressing the intracellular cGAS-STING-mediated inflammatory pathways, and ultimately contributed to the progression of neuronal loss in neurodegenerative disorders such as Parkinson disease [18].

Selenium (Se) was one of the indispensable trace elements inside human body which was closely related with a variety of physiological functions. As the main form of selenium consumed by humans, selenomethionine was mainly intaked through diet, such as vegetables, seafood, meat and dairy products [19]. It was widely known that selenium could reduce inflammation, enhance immunity, promote antioxidation, and then prevent many related diseases [20]. Especially, the anti-inflammatory effect of selenium is closely related to the suppression of NF-κB. Mou et al. found that as an organic Se source, maternal 2-hydroxy-4-methylselenobutanoic acid (HMSeBA) supplementation significantly suppressed the expression of ileal IL-1β, IL-6 and NF-κB genes in newborn piglets compared with the control group, and thus protected against inflammation in the gut [21]. Tang et al. found that Se deficiency induced a redox imbalance in the liver of pigs, and led to increased levels of hepatic pro-inflammatory factors by activating the NF-κB pathway [22]. Zhang et al. found that a Se-supplemented diet significantly inhibited the phosphorylation of NF-κB and MAPKs signaling pathway in mammary tissues of BALB/c mice and

primary mouse mammary epithelial cells (MMECs), which contributed to inhibit inflammation in *Staphylococcus aureus* (*S. aureus*)-induced mastitis in mice [23].

Until now, the role and involved mechanism of inflammatory response in the senescence of pneumonocytes during exposure to $PM_{2.5}$ has not been fully clarified. Therefore, in our study, to understand whether this issue is related to the activation of cGAS/STING/NF-κB pathway and selenium can antagonize $PM_{2.5}$-induced senescence of pneumonocytes by inhibiting this pathway, A549 pretreated with selenomethionine were exposed to specified concentrations of $PM_{2.5}$, and assayed for senescence-related endpoints. This study will help us to establish a theoretical basis of optimizing the prevention and control scheme of $PM_{2.5}$.

Materials And Methods

Preparation and treatment of $PM_{2.5}$

The A549 cell line, was maintained in complete DMEM medium (Gibco, New York, USA) supplemented with 10% fetal bovine serum (FBS) and 1% antibiotics (100 U/mL penicillin and 100 μg/mL streptomycin). A549 cells were cultured at 37°C in a humidified 5% CO_2 atmosphere and passaged at confluent condition. The powder of $PM_{2.5}$ was prepared from standard reference material 1649b (SRM 1649b) which were composed of urban dust purchased from National Institute of Standards and Technology (NIST, Gaithersburg, USA). A total of 50 mg PMs were dispersed in 1 mL dimethyl sulfoxide (DMSO, purity ≥ 99.0%, Sangon Biotech, Shanghai, China), shaken, and ultra-sonicated for 24 h in an ultrasonic bath. Afterwards, 2 μL stock solutions were dispersed in 1 mL ultrapure water for particle-size analysis using a Zetasizer Nano ZS90 zeta Potentiometer (Malvern Panalytical, Malvern, UK), and a stock solution at a concentration of 50 mg/mL were stored at 25°C in the dark. Before the preparation of working solution, ultrasonic vibration was performed for 2 h to ensure that it is a uniformly dispersed suspension. Working solutions at graded concentrations (25, 50 and 100 μg/mL) were prepared by diluting the stock solution with complete DMEM medium. Then, A549 cells were treated with working solution at graded concentrations (25, 50 and 100 μg/mL) and vehicle (0.2% DMSO) for 24 and 48 h. A549 cells without any treatment were used as the control. After treatment, A549 cells were adopted for further studies.

Cell Viability Assay

The cytotoxic effect of $PM_{2.5}$ on A549 cells was evaluated by MTT assay. Briefly, A549 cells were seeded at a density of 1×10^4 cells per well into a 96-well microtiter plate and cultured for 24 h, allowing cells to adhere to the bottom of 96-well microtiter plate. After A549 cells were treated with 25-100 μg/mL $PM_{2.5}$ and 0.2% DMSO for 24 and 48 h, 1 g/L 3-(4,5-dimethylthiazol-2-yl)-2,5-diphenyltetrazolium bromide (MTT, Sangon Biotech, Shanghai, China) working solution was added to replace the growth medium, and the cultures were further incubated in dark at 37°C for 4 h. Afterwards, the supernatant was removed and 200 μL DMSO was added to dissolve the formed formazan crystals. The optical density (OD) was

recorded at an absorbance wavelength of 490 nm using a SpectraMax M5 fluorescence reader (Molecular Devices, Sunnyvale, USA).

Cell Cycle Analysis

Cell cycle was detected by flow cytometry using Cell Cycle Analysis Kit (Beyotime, Shanghai, China) as manufacturer's protocol. Briefly, after exposure to 25-100 μg/mL $PM_{2.5}$ and 0.2% DMSO for 24 and 48 h, A549 cells were trypsinized and washed twice with PBS. Afterwards, the treated cells were fixed by 1 mL 70% pre-cooled ethanol overnight at 4°C and subsequently incubated with 500 μL propidium iodide (PI) working solution (20 μg/mL PI and 10 μg/mL RNase) for 30 min at 37°C in the dark. Finally, the distribution in the cell cycle was detected using CytoFLEX flow cytometer (Beckman Coulter, Brea, USA) and analyzed by FlowJo software. Cell cycle was evaluated according to the distribution of DNA content and divided into sub-G1, G1, S and G2/M phases.

Senescence-associated β-galactosidase optical staining

Senescence-associated β-galactosidase (SA-β-gal) activity was detected using Senescence β-Galactosidase Staining Kit (Beyotime, Shanghai, China) as manufacturer's protocol. Briefly, A549 cells were seeded at a density of 1×10^5 cells per well in a 12-well microtiter plate and exposed to 25-100 μg/mL $PM_{2.5}$ and 0.2% DMSO for 24 and 48 h. Then, the treated cells were incubated with fixative working solution for 15 min at 25°C. Afterwards, A549 cells were stained with β-galactosidase staining solution overnight at 37°C under the condition of CO_2-free. Images were taken in five random fields using optical microscope and analyzed with Image J software.

Senescence-associated β-galactosidase fluorescent staining

Senescence-associated β-galactosidase (SA-β-gal) activity was detected using CellEvent™ Senescence Green Detection Kit (ThermoFisher Scientific, Waltham, USA) as manufacturer's protocol. Briefly, A549 cells were cultured on microscope cover glass in a 6-well microtiter plate for 24 h and treated with 25-100 μg/mL $PM_{2.5}$ and 0.2% DMSO for 24 and 48 h. Then, the treated cells were fixed with 4% paraformaldehyde for 30 min at 25°C. After rinsed three times with 1% bovine serum albumin (BSA) in PBS, cells were incubated in dark with β-galactosidase staining solution under the condition of CO_2-free. Afterwards, cells were incubated with 1 μg/mL Hoechst 33342 nuclear stain (Molecular Probes, Waltham, USA) for 8 min. Finally, the microscope cover glass were mounted at glass slides and analyzed by LSM710 laser scanning confocal microscope (Carl Zeiss, Oberkohen, Germany). At least 1000 cells were scored, and the fluorescence intensity in A549 cells with β-galactosidase foci per 1000 cells were quantitatively analyzed based on each independent experiment.

Western blot assay

The protein expression of γ-H2AX, cGAS, STING, phospho-NF-κB (p-p65), TNF-α, IL-6, IL-8, p16 and p21 was determined by Western blot. Briefly, after A549 cells were treated with $PM_{2.5}$ in 60-mm dishes, total

proteins were harvested by lysing in ice-cold RIPA lysis buffer containing 1 mM PMSF (Beyotime, Shanghai, China). The concentration of total proteins was measured by Pierce™ BCA Protein Assay Kit (ThermoFisher Scientific, Waltham, USA). Equal amounts of proteins were separated by 10% SDS-PAGE gel and electrophoretically transferred to a polyvinylidene fluoride (PVDF) membrane. After blocking with 5% non-fat milk or BSA in TBST for 90 min at 25°C, the PVDF membrane was overnight incubated by employing primary antibodies of γ-H2AX (1:2000, Millipore, Billerica, USA), cGAS (1:1000, Cell Signaling Technology, Danvers, USA), STING (1:1000, Cell Signaling Technology, Danvers, USA), p-p65 (1:5000, Cell Signaling Technology, Danvers, USA), TNF-α (1:2000, Abcam, Cambridge, UK), IL-6 (1:1000, Abcam, Cambridge, UK), IL-8 (1:1000, Abcam, Cambridge, UK), p16 (1:2000, Cell Signaling Technology, Danvers, USA), p21 (1:2000, Cell Signaling Technology, Danvers, USA) and β-actin (1:2000, TransGen, Beijing, China) at 4°C. Afterwards, the PVDF membrane was subsequently incubated with HRP-conjugated secondary antibodies (1:5000, TransGen, Beijing, China) for 1 h at 25°C. β-actin was used as the internal control. The images of protein bands were visualized using an enhanced chemiluminescence (ECL) detection system. Densitometric analysis of the images was performed with Image J software.

Immunofluorescent assay

The activation of cGAS was assessed by immunofluorescent assay. Briefly, A549 cells were cultured on microscope cover glass in a 6-well microtiter plate for 24 h and treated with 100 μg/mL $PM_{2.5}$ and 0.2% DMSO for 48 h. After fixing with 4% paraformaldehyde for 30 min at 25°C and permeabilizing with 0.5% Triton X-100 in PBS for 30 min at 25°C, the treated cells were blocked with 5% BSA in 0.1% Triton X-100 for another 1 h at 25°C, followed by employing primary antibody of γ-H2AX (1:1000, Novus Biologicals, Littleton, New Zealand) for 2 h at 25°C. Afterwards, cells were blocked with 5% non-fat milk in 0.1% Triton X-100 for 1 h at 25°C before incubating by employing primary antibody of cGAS (1:1000, Cell Signaling Technology, Danvers, USA) overnight at 4°C. Finally, after incubating by employing secondary antibody of Alexa Fluor 488-conjugated goat anti-rabbit IgG (1:2000, TransGen, Beijing, China) and Alexa Fluor 555-conjugated donkey anti-mouse IgG (1:2000, TransGen, Beijing, China) for 2 h at 25°C, nuclei were counterstained with 1 μg/mL DAPI for 10 min at 25°C. Images were captured using a LSM710 laser scanning confocal microscope (Carl Zeiss, Oberkohen, Germany) and processed with a LSM image browser.

Treatment with cGAS and NF-κB inhibitor, and pretreatment with Se-Met

A549 cells were exposed to 100 μg/mL $PM_{2.5}$ with 10 μM PF-06928215 (a inhibitor of cGAS, MedChemExpress, New Jersey, USA) or 5 μM BAY 11-7082 (a inhibitor of NF-κB, MedChemExpress, New Jersey, USA) for 48 h. In addition, 20 μM selenomethionine (Se-Met, Macklin, Shanghai, China) was prepared to pretreat exponentially growing A549 cells for 12 h. Afterwards, treated cells were used to determine the expression level of cGAS/STING/NF-κB pathway- and senescence-related proteins, as well as the percentage of SA-β-gal-positive cells and fluorescence intensity of SA-β-gal foci as described above.

Statistical analysis

Data from at least three independent experiments were performed for statistical analysis and presented as mean ± S.D. Statistical significance between different groups was assessed using one-way analysis of variance (ANOVA) with Fisher's least significant difference test. The value of $p < 0.05$ was considered to indicate a statistically significant difference (*).

Results

$PM_{2.5}$ delayed the growth of A549 cells

The analysis of particle-size distribution showed that the particle-size range of a stock solution of PMs after ultrasonication was totally between 1.0 and 1.9 μm, which was identified as $PM_{2.5}$ (Fig. S1). MTT assay was used to evaluate the effect of $PM_{2.5}$ on the viability of A549 cells. As shown in Fig. 1A, when A549 cells were treated with 50 and 100 μg/mL $PM_{2.5}$ for 24 h, the survival fraction was significantly reduced to 80.74 ± 2.16% and 77.97 ± 1.97% compared to the untreated cells ($p < 0.01$). Meanwhile, after the treatment with 50 and 100 μg/mL $PM_{2.5}$ for 48 h, the survival fraction of A549 cells was further remarkably decreased to 78.35 ± 2.09% and 73.31 ± 1.71% ($p < 0.01$). To ascertain the influence on cell cycle, flow cytometric method was adopted to show that exposure to $PM_{2.5}$ could lead to G2/M phase arrest (Figs. 1B and C). When A549 cells were treated with 50 and 100 μg/mL $PM_{2.5}$ for 24 h, the percentage of cells in G2/M phase was significantly increased to 11.86 ± 1.37% ($p < 0.05$) and 11.49 ± 0.84% ($p < 0.01$) from 8.48 ± 0.96% in the control group. Additionally, the treatment with 50 and 100 μg/mL $PM_{2.5}$ for 48 h raised the percentage of cells in G2/M phase to 13.10 ± 1.11% ($p < 0.01$) and 15.34 ± 1.42% ($p < 0.01$) relative to 7.53 ± 0.54% in the untreated group, respectively. These results implied that $PM_{2.5}$ induced cell cycle arrest in G2/M phase due to the cytotoxic potential to A549 cells.

$PM_{2.5}$ induced the senescence of alveolar epithelial cells

The elevated activity of SA-β-gal and increased protein expression of intracellular senescence marker (p16 and p21) was universally regarded as common features of senescent cells [24]. As shown in Figs. 2A-C, compared with the corresponding controls, after exposure to 50 and 100 μg/mL $PM_{2.5}$ for 48 h, the protein expression of p16 detected by Western blot was significantly increased to 1.52 ± 0.35-fold ($p < 0.05$) and 1.78 ± 0.47-fold ($p < 0.01$), the protein level of p21 was also dramatically elevated to 1.73 ± 0.36-fold ($p < 0.01$) and 1.75 ± 0.22-fold ($p < 0.01$), but there was no significant change in the protein expressions of p16 and p21 in A549 cells exposed to $PM_{2.5}$ for 24 h. Moreover, to further ascertain the occurrence of senescence caused by $PM_{2.5}$, the percentage of SA-β-gal-positive cells was also examined. It was found that $PM_{2.5}$ induced the increased percentage of SA-β-gal-positive cells with time- and dose-dependency. When A549 cells were treated with 50 and 100 μg/mL $PM_{2.5}$ for 48 h, the percentage of SA-β-gal-positive cells was remarkably increased to 11.24 ± 0.50% and 16.01 ± 0.78% from 2.55 ± 0.36% in the control group (Figs. 2D and E, $p < 0.01$). We also calibrated the fluorescence images of SA-β-gal foci

in A549 cells exposed to $PM_{2.5}$. The results showed that exposure to 50 and 100 μg/mL $PM_{2.5}$ for 48 h significantly enhanced the fluorescence intensity to 7.25 ± 1.87-fold and 11.33 ± 2.88-fold compared to the control group (Fig. S2, $p < 0.01$). These data collaboratively suggested that $PM_{2.5}$ could lead to the occurrence of cellular senescence in A549 cells in a time- and concentration-dependent manner.

$PM_{2.5}$ led to DNA damage and activated cGAS/STING pathway

As a typical biomarker of DNA damage, the phosphorylated histone H2AX (γ-H2AX) was examined by Western blot to explore the effect of $PM_{2.5}$ on DNA double-strand breaks in A549 cells. As shown in Figs. 3A and B, the protein expression of γ-H2AX in A549 cells treated with 50 and 100 μg/mL $PM_{2.5}$ for 48 h was significantly increased to 1.66 ± 0.15-fold ($p < 0.01$) and 2.16 ± 0.26-fold ($p < 0.01$) in contrast to that in the control group. Furthermore, due to that cGAS/STING pathway has been demonstrated to respond to cytoplasmic DNA fragment, the protein expression of cGAS and STING was also determined. From Figs. 3A and C shown, it was found that when A549 cells were treated with 50 and 100 μg/mL $PM_{2.5}$ for 48 h, compared to the untreated control, the protein expression of cGAS was remarkably increased to 2.03 ± 0.53-fold ($p < 0.01$) and 2.18 ± 0.47-fold ($p < 0.01$), and the protein level of STING was also significantly elevated to 1.69 ± 0.32-fold ($p < 0.01$) and 1.75 ± 0.41-fold ($p < 0.01$). Additionally, to further corroborate above fact, immunofluorescent assay was adopted to detect the colocalization of cytoplasmic DNA foci, γ-H2AX and cGAS. As shown in Fig. 3D, staining of A549 cells with DAPI and anti-γ-H2AX antibody revealed that $PM_{2.5}$-induced damaged DNA was accumulated in the cytoplasm. Meanwhile, it was also observed that $PM_{2.5}$ led to the formation of cGAS that colocalized with cytoplasmic DNA foci. These phenomena jointly indicated that $PM_{2.5}$ activated cGAS/STING pathway through sensing cytoplasmic DNA fragment caused by DNA double-strand breaks.

$PM_{2.5}$-induced senescence of alveolar epithelial cells was regulated by inflammation

To study the role of inflammation in $PM_{2.5}$-induced cellular senescence, Western blot was adopted to detect the protein expression of p-p65, TNF-α, IL-6 and IL-8. When A549 cells were treated with 50 and 100 μg/mL $PM_{2.5}$ for 48 h, the protein expression of p-p65 was remarkably increased to 1.70 ± 0.43-fold ($p < 0.05$) and 1.78 ± 0.19-fold ($p < 0.05$) compared with that in the control (Figs. 4A and B). Meanwhile, as shown in Figs. 4A and C, compared to the untreated group, the treatment of 50 μg/mL $PM_{2.5}$ significantly elevated the protein expression of TNF-α, IL-6 and IL-8 to 2.09 ± 0.61-fold ($p < 0.01$), 2.18 ± 0.52-fold ($p < 0.05$) and 2.11 ± 0.54-fold ($p < 0.05$), and exposure to 100 μg/mL $PM_{2.5}$ also remarkably increased the protein level of TNF-α, IL-6 and IL-8 to 2.69 ± 0.79 ($p < 0.01$), 2.69 ± 0.89-fold ($p < 0.01$) and 2.66 ± 0.35-fold ($p < 0.05$).

Furthermore, to investigate the regulatory mechanism of cGAS/STING/NF-κB pathway in inflammation and senescence induced by $PM_{2.5}$, PF-06928215 (cGAS inhibitor) and BAY 11-7082 (NF-κB inhibitor) was used to clarify this issue. With the addition of BAY 11-7082, the protein expression of TNF-α, IL-6 and IL-8 in A549 cells exposed to 100 μg/mL $PM_{2.5}$ for 48 h was significantly reduced to 1.70 ± 0.55-fold ($p <$

0.01), 1.26 ± 0.37-fold ($p < 0.05$) and 2.78 ± 0.37-fold ($p < 0.05$) from 2.79 ± 0.70-fold, 2.29 ± 0.68-fold and 5.15 ± 1.24-fold, respectively (Figs. 5A and C). Moreover, it was also found that compared to alone exposure to 100 μg/mL $PM_{2.5}$, a significant reduction in the protein expression of p16 and p21 (Figs. 5A and D) and the percentage of SA-β-gal-positive cells (Figs. 5E and F) was also detected in A549 cells concurrently exposed to 100 μg/mL $PM_{2.5}$ and 5 μM BAY 11-7082 for 48 h, which demonstrated that the occurrence of senescence in alveolar epithelial cells exposed to $PM_{2.5}$ was closely associated with inflammatory response. In addition, when A549 cells were concurrently exposed to 100 μg/mL $PM_{2.5}$ and 10 μM PF-06928215 for 48 h, compared to alone exposure to 100 μg/mL $PM_{2.5}$, the protein expression of STING, p-p65, TNF-α, IL-6 and IL-8 was remarkably reduced to 1.01 ± 0.27-fold ($p < 0.05$), 1.19 ± 0.31-fold ($p < 0.05$), 1.82 ± 0.70-fold ($p < 0.01$) , 1.35 ± 0.72-fold ($p < 0.05$) and 2.85 ± 0.73-fold ($p < 0.05$) from 1.55 ± 0.35-fold, 3.09 ± 0.25-fold, 2.79 ± 0.70-fold, 2.29 ± 0.68-fold and 5.15 ± 1.24-fold (Figs. 5A-C), the protein level of p16 and p21 was also significantly decreased to 1.36 ± 0.76-fold ($p < 0.01$) and 1.86 ± 0.93-fold ($p < 0.05$) from 3.53 ± 0.52-fold and 2.88 ± 0.86-fold (Figs. 5A and D), meanwhile, the percentage of SA-β-gal-positive cells was found to decrease from 16.01 ± 0.78% to 10.17 ± 0.54% (Figs. 5E and F, $p < 0.01$). These above results illustrated that $PM_{2.5}$-induced cellular senescence in alveolar epithelial cells was mainly regulated by inflammation triggered through cGAS/STING/NF-κB pathway.

Se-Met inhibited $PM_{2.5}$-induced inflammation mediated by cGAS/STING/NF-κB pathway

To show the effect of Se-Met on $PM_{2.5}$-induced activation of cGAS/STING/NF-κB pathway, A549 cells pretreated with 20 μM Se-Met for 12 h were then exposed to 100 μg/mL $PM_{2.5}$ for 48 h, and detected for the protein expression of cGAS, STING, p-p65, TNF-α, IL-6 and IL-8. It was found that in contrast to alone exposure to $PM_{2.5}$, Se-Met pretreatment significantly reduced the protein expression of cGAS, STING and p-p65 to 0.77 ± 0.44-fold, 1.41 ± 0.28-fold and 1.28 ± 0.15-fold from 1.83 ± 0.72-fold, 1.95 ± 0.46-fold and 1.60 ± 0.25-fold, respectively (Figs. 6A-D, $p < 0.05$). In the meantime, after the pretreatment with 20 μM Se-Met, the protein expression of TNF-α, IL-6 and IL-8 in A549 cells exposed to 100 μg/mL $PM_{2.5}$ was also remarkably decreased to 0.91 ± 0.18-fold ($p < 0.01$), 1.02 ± 0.25-fold ($p < 0.05$) and 1.86 ± 0.53-fold ($p < 0.01$) from 1.89 ± 0.18-fold, 1.50 ± 0.24-fold and 2.83 ± 0.77-fold, respectively (Figs. 6A and E). These data suggested that Se-Met could attenuate inflammation induced by $PM_{2.5}$ through hindering cGAS/STING/NF-κB pathway in alveolar epithelial cells.

Se-Met prevented $PM_{2.5}$-induced senescence of alveolar epithelial cells

To clarify the effect of Se-Met on $PM_{2.5}$-induced cellular senescence, the activity of SA-β-gal and protein expression of p16 and p21 in A549 cells pretreated with 20 μM Se-Met for 12 h was determined after exposure to 100 μg/mL $PM_{2.5}$ for 48 h. As shown in Figs. 7A and B, it was found that compared to alone exposure to $PM_{2.5}$, the protein expression of p16 and p21 after Se-Met pretreatment was remarkably decreased to 1.16 ± 0.12-fold and 2.41 ± 0.37-fold from 1.60 ± 0.16-fold and 4.00 ± 0.34-fold, respectively ($p < 0.05$). Moreover, with the pretreatment of Se-Met, the percentage of SA-β-gal-positive cells in A549

cells exposed to 100 μg/mL $PM_{2.5}$ was significantly decreased to 10.79 ± 1.04% from 16.01 ± 0.78% (Figs. 7C and D, $p < 0.01$). We also calibrated the fluorescence images of SA-β-gal foci in A549 cells, which indicated that Se-Met pretreatment significantly decreased the fluorescence intensity to 6.67 ± 1.71-fold as compared to 12.17 ± 3.72-fold in alone treatment with $PM_{2.5}$ (Fig. S3, $p < 0.05$). These results jointly corroborated that Se-Met could protect alveolar epithelial cells from the occurrence of cellular senescence after exposure to $PM_{2.5}$.

Discussion

Nowadays, airborne $PM_{2.5}$ have attracted a major concern for public health. Moreover, $PM_{2.5}$ has characteristics of long retention time and transmission distance in the air, and is liable to cause serious harm to lung organ in human [25, 26]. In previous studies, A549 cell line has been widely used as alveolar epithelial cell model to study the effects of different toxic chemicals on the senescence in lung organ. For instance, Gao et al. shown that $β_2M$ increased in plasma and lung tissues of emphysema induced a cellular senescence phenotype in A549 cells to participate in cigarette smoke extract (CSE)-induced lung emphysema [27]. Hyzdalova et al. found that two-week exposure of A549 to benzo[α]pyrene (B[a]P) significantly inhibited cell proliferation, induced increased number of senescent cells, and promoted p21-dependent epithelial-to-mesenchymal transition (EMT)-like phenotype [28]. Chen et al. also found that when exposure to diesel exhaust particles (DEPs), the reduced expression of inter-alpha-trypsin inhibitor heavy chain 4 (ITIH4) as a type II acute-phase protein could be a vital reason for the senescence of alveolar epithelial (A549) cells [29]. Here, it was indicated that $PM_{2.5}$ induced the senescence-like phenotype of A549 cells in a time- and concentration-dependent manner, as evidenced by the cell cycle arrest in G2/M phase, the elevated protein level of p16 and p21, the increased percentage of SA-β-gal-positive cells (Figs. 1 and 2) and fluorescence intensity of SA-β-gal foci (Fig. S2). In addition, previous studies have shown that inflammation was closely associated with cellular senescence. Kang et al. found that the blockage of p62-dependent autophagic degradation of GATA4 activated NF-κB inflammatory response, and then initiated the SASP and resulted in increased SA-β-gal-positive senescent cells [5]. Tezze et al. found that acute deletion of optic atrophy 1 (OPA1) with tamoxifen in adult mice induced high inflammatory cytokines such as IL-6, IL-1α, IL-1β and TNF-α in blood, eventually led to significant increasement of β-galactosidase and p21 in liver, skin and gut [30]. Jurk et al. found that chronic, progressive low-grade inflammation induced by knockout of nfkb1 induced premature aging in mice by aggravating mitochondrial ROS production via COX-2 activation and, consequently, enhancing nuclear DNA damage response (DDR) [31].

As a stress response of lung organ to external stimuli, inflammation caused by lifelong chronic antigen stimulation and oxidative stress would promote age-related changes in innate and adaptive immune responses and lead to a variety of lung diseases, such as COPD, IPF, ARDS and community-acquired pneumonia (CAP) [32]. Due to the potent proinflammatory potential, cytokines such as TNF-α, IL-6 and IL-8 were commonly manifested as the inflammatory markers [33]. Kanderova et al. treated THP-1 cells stably expressing wild-type hematopoietic cell kinase (HCK^{WT}) and mutant hematopoietic cell kinase

(HCK^{MUT}, lacks the C-terminal tail including Tyr522, which was predicted to result in hyperactivation of HCK) with lipopolysaccharide (LPS) and found that the LPS-activated THP-1 HCK^{MUT} cells produced more IL-6, IL-8, TNF-α and IL-1β than THP-1 HCK^{WT} cells, which might ultimately resulted in inflammation observed in patients with early-onset pulmonary and cutaneous vasculitis [34]. Finney et al. found when alveolar macrophages and monocyte-derived macrophages (MDM) from patients with COPD were infected with human rhinovirus 16 (HRV16), the release of IL-8, IL-6, TNF-α and IL-10, and phagocytosis of *H. influenzae* and *S. pneumoniae* was both impaired, suggesting that HRV16 increased susceptibility to secondary bacterial infection and promoted resolution of inflammation, eventually leading to prolonged exacerbations in COPD [35]. In our study, it was also found that when A549 cells were exposed to 50 and 100 μg/mL $PM_{2.5}$ for 48 h, the protein expression of TNF-α, IL-6 and IL-8 was remarkably promoted compared to that in the corresponding control (Figs. 4A and C). It is tempting to postulate that $PM_{2.5}$-induced senescence of alveolar epithelial cells was regulated by inflammatory response.

As a pivotal regulator of various immune responses, NF-κB promoted the activation of lymphocytes and leukocytes by regulating the expression of pro-inflammatory cytokines, such as IL-1, IL-6, IL-8 and TNF-α [36]. Additionally, the constitutive activation of NF-κB signaling pathway was often associated with some monogenic diseases, such as immunodeficiency, developmental disorders and cancer [37]. In normal cells, NF-κB resided predominantly in the cytoplasm in a complex with inhibitory IκB proteins. When signaling pathways were activated, the IκB proteins were degraded by phosphorylation and subsequent ubiquitination under the action of IκB kinase (IKK), and also NF-κB dimers entered the nucleus to modulate target gene expression [38]. Our data showed that exposure to 50 and 100 μg/mL $PM_{2.5}$ for 48 h elevated the protein expression of p-p65, which indicated that NF-κB was activated (Figs. 4A and B). Besides, numerous studies have suggested that the cytosolic DNA-sensing pathway through cGAS plays a major role in the cellular inflammatory response [39]. Bai et al. found that disulfide-bond A oxidoreductase-like protein (DsbA-L) deficiency promoted mtDNA release into the cytosol, thereby triggered inflammatory responses by activating the DNA-sensing cGAS-cGAMP-STING pathway [40]. Yu et al. found that pharmacologic inhibition or genetic deletion of cGAS and its downstream signaling partner STING prevented upregulation of NF-kB and type I IFN induced by TDP-43 in induced pluripotent stem cell (iPSC)-derived motor neurons and in TDP-43 mutant mice [41]. Here, we also found that 48 h-exposure to 50 and 100 μg/mL $PM_{2.5}$ induced the remarkable upregulation of γ-H2AX, cGAS and STING proteins in A549 cells (Fig. 3). Furthermore, using PF-06928215 as a inhibitor of cGAS, our study found that compared to alone exposure to $PM_{2.5}$, the protein expression of STING, p-p65, TNF-α, IL-6 and IL-8 in A549 cells was all significantly decreased after concurrent treatment with 100 μg/mL $PM_{2.5}$ and 10 μM PF-06928215 for 48 h (Figs. 5A-C). It was also found that 5 μM BAY 11-7082 as a inhibitor of NF-κB dramatically decreased the protein level of TNF-α, IL-6 and IL-8 when A549 cells were exposed to 100 μg/mL $PM_{2.5}$ for 48 h (Figs. 5A and C). Meanwhile, it was demonstrated that the inhibition of cGAS and NF-κB could remarkably decreased amounts of p16 and p21 (Figs. 5A and D), and reduced the percentage of SA-β-gal-positive cells (Figs. 5E and F). These above results jointly proved that cGAS-

dependent inflammatory response mediated by NF-κB might be crucial for $PM_{2.5}$-induced senescence of alveolar epithelial cells.

Recent studies have suggested that selenium supplementation was closely associated with the prevention of many diseases, such as cognitive decline, poor fertility, autoimmune thyroid disease, cardiovascular disease, cancer and type-2 diabetes [42]. In addition, it was noteworthy that these harmful symptoms were essentially demonstrated to be caused by cellular senescence [43]. Therefore, the therapeutic mechanism of selenium on cellular senescence has been receiving special attention in the past. Jobeili et al. found that sodium selenite supplementation extended the replicative lifespan and delayed skin equivalent senescence by activating adhesion to type IV collagen and laminin 332 of human primary keratinocytes [44]. Lee et al. also found that the loss of selenoprotein caused by alkylation repair homolog 8 (ALKBH8) deficiency in MEFs limited H_2O_2 removal and exacerbated cellular senescence, which reminded that selenium supplementation might be useful as a novel strategy for delaying senescence [45]. Hammad et al. proved that selenium supplementation in the culture media improved the replicative potential and reduce senescence-associated heterochromatin foci (SAHF) of WI-38 cells, accompanied by an increased expression of almost all selenoproteins [46]. To sum up, the beneficial effects of selenium on alleviating senescence were multiple and complex. In this study, we observed that 20 μM Se-Met pretreatment significantly inhibited the expression of cGAS/STING/NF-κB pathway-related proteins in A549 cells exposed to 100 μg/mL $PM_{2.5}$ for 48 h (Fig. 6). Moreover, the protein level of p16 and p21, the percentage of SA-β-gal-positive cells (Fig. 7) and fluorescence intensity of SA-β-gal foci (Fig. S3) was also remarkably decreased when A549 cells pretreated with 20 μM Se-Met were exposed to 100 μg/mL $PM_{2.5}$ for 48 h. These conclusions suggested that selenium protected against $PM_{2.5}$-induced senescence of alveolar epithelial cells by attenuating inflammatory response mediated by cGAS/STING/NF-κB pathway.

In conclusion, our data provided corroborative information that Se-Met inhibited $PM_{2.5}$-induced inflammatory response regulated by cGAS/STING/NF-κB pathway, and then prevented the senescence of alveolar epithelial cells. Since $PM_{2.5}$ has been ubiquitously detected in the atmosphere, and also it was widely known that cellular senescence was a potential risk factor for human health and life span, our study provided a theoretical basis for better understanding the harmful effect caused by $PM_{2.5}$ and establishing the prevention and control program of atmospheric pollution.

Declarations

Acknowledgements

Not applicable.

Authors' contributions

Xiaofei Wang and Xuanyi Xia conceived the study and drafted the article. Xiaofei Wang, Xuanyi Xia, Wenzun Lu and Yuchen Zhu performed experiments and analyzed data. Chunmei Ge, Xiaoying Guo and Ning Zhang revised the article. Hua Chen and Shengmin Xu performed the analysis with constructive discussions. All authors read and approved the final manuscript.

Funding

This study was supported by the Key Project of Natural Science Research of Anhui High Education Institutions (No. KJ2020A0665), the Natural Science Foundation of Anhui Province (No. 2108085MB41), the Open Fund of Information Materials and Intelligent Sensing Laboratory of Anhui Province (No. IMIS202006), the National First-Class Discipline Program of Bioengineering at Hefei University (No. 12612001130), the Talent Research Foundation of Hefei University (No. 20RC38), and the Open Fund of Key Laboratory of Rural Renewable Energy Development and Utilization in Ministry of Agriculture (No. 2018-007).

Availability of data and materials

Datasets generated for this study are available from the corresponding author upon reasonable request.

Ethics approval and consent to participate

Not applicable.

Consent for publication

Not applicable.

Competing interests

The authors declare no competing financial interest.

References

1. Karottki DG, Spilak M, Frederiksen M, Gunnarsen L, Brauner EV, Kolarik B, et al. An indoor air filtration study in homes of elderly: cardiovascular and respiratory effects of exposure to particulate matter. Environ Health. 2013;12:116.
2. Myhre O, Lag M, Villanger GD, Oftedal B, Ovrevik J, Holme JA, et al. Early life exposure to air pollution particulate matter (PM) as risk factor for attention deficit/hyperactivity disorder (ADHD): Need for novel strategies for mechanisms and causalities. Toxicol Appl Pharmacol. 2018;354:196–214.
3. Xing YF, Xu YH, Shi MH, Lian YX. The impact of PM2.5 on the human respiratory system. J Thorac Dis. 2016;8:E69-74.
4. Meyer KC, M.D., M.S., F.A.C.P., F.C.C.P. The role of immunity and inflammation in lung senescence and susceptibility to infection in the elderly. Semin Respir Crit Care Med. 2010;31:561–74.

5. Kang C, Xu Q, Martin TD, Li MZ, Demaria M, Aron L, et al. The DNA damage response induces inflammation and senescence by inhibiting autophagy of GATA4. Science. 2015;349:aaa5612.
6. Chilosi M, Carloni A, Rossi A, Poletti V. Premature lung aging and cellular senescence in the pathogenesis of idiopathic pulmonary fibrosis and COPD/emphysema. Transl Res. 2013;162:156–73.
7. Dominici F, Peng RD, Bell ML, Pham L, McDermott A, Zeger SL, et al. Fine particulate air pollution and hospital admission for cardiovascular and respiratory diseases. JAMA. 2006;295:1127–34.
8. Winterbottom CJ, Shah RJ, Patterson KC, Kreider ME, Panettieri RA, Jr., Rivera-Lebron B, et al. Exposure to Ambient Particulate Matter Is Associated With Accelerated Functional Decline in Idiopathic Pulmonary Fibrosis. Chest. 2018;153:1221–28.
9. Young AR, Narita M. SASP reflects senescence. EMBO Rep. 2009;10:228–30.
10. Rodier F, Campisi J. Four faces of cellular senescence. J Cell Biol. 2011;192:547–56.
11. Han L, Zhang Y, Zhang M, Guo L, Wang J, Zeng F, et al. Interleukin-1beta-Induced Senescence Promotes Osteoblastic Transition of Vascular Smooth Muscle Cells. Kidney Blood Press Res. 2020;45:314–30.
12. Gao C, Ning B, Sang C, Zhang Y. Rapamycin prevents the intervertebral disc degeneration via inhibiting differentiation and senescence of annulus fibrosus cells. Aging (Albany NY). 2018;10:131–43.
13. Tichy ED, Ma N, Sidibe D, Loro E, Kocan J, Chen DZ, et al. Persistent NF-kappaB activation in muscle stem cells induces proliferation-independent telomere shortening. Cell Rep. 2021;35:109098.
14. Hopfner KP, Hornung V. Molecular mechanisms and cellular functions of cGAS-STING signalling. Nat Rev Mol Cell Biol. 2020;21:501–21.
15. Loo TM, Miyata K, Tanaka Y, Takahashi A. Cellular senescence and senescence-associated secretory phenotype via the cGAS-STING signaling pathway in cancer. Cancer Sci. 2020;111:304–11.
16. Li. T, Chen ZJ. The cGAS-cGAMP-STING pathway connects DNA damage to inflammation, senescence, and cancer. J Exp Med. 2018;215:1287–99.
17. Bi X, Du C, Wang X, Wang XY, Han W, Wang Y, et al. Mitochondrial Damage-Induced Innate Immune Activation in Vascular Smooth Muscle Cells Promotes Chronic Kidney Disease-Associated Plaque Vulnerability. Adv Sci (Weinh). 2021;8:2002738.
18. Kwon OC, Song JJ, Yang Y, Kim SH, Kim JY, Seok MJ, et al. SGK1 inhibition in glia ameliorates pathologies and symptoms in Parkinson disease animal models. EMBO Mol Med. 2021;13:e13076.
19. Avery JC, Hoffmann PR. Selenium, Selenoproteins, and Immunity. Nutrients. 2018;10:1203.
20. Huang Z, Rose AH, Hoffmann PR. The role of selenium in inflammation and immunity: from molecular mechanisms to therapeutic opportunities. Antioxid Redox Signal. 2012;16:705–43.
21. Mou D, Ding D, Yang M, Jiang X, Zhao L, Che L, et al. Maternal organic selenium supplementation during gestation improves the antioxidant capacity and reduces the inflammation level in the

intestine of offspring through the NF-kappaB and ERK/Beclin-1 pathways. Food Funct. 2021;12:315–27.

22. Tang C, Li S, Zhang K, Li J, Han Y, Zhan T, et al. Selenium deficiency-induced redox imbalance leads to metabolic reprogramming and inflammation in the liver. Redox Biol. 2020;36:101519.
23. Zhang Z, Guo YF, Li CY, Qiu CW, Guo MY. Selenium influences mmu-miR-155 to inhibit inflammation in Staphylococcus aureus-induced mastitis in mice. Food Funct. 2019;10:6543–55.
24. Campisi J. Aging, cellular senescence, and cancer. Annu Rev Physiol. 2013;75:685–705.
25. Niu J, Liberda EN, Qu S, Guo X, Li X, Zhang J, et al. The role of metal components in the cardiovascular effects of PM2.5. PLoS One. 2013;8:e83782.
26. Yang L, Wang WC, Lung SC, Sun Z, Chen C, Chen JK, et al. Polycyclic aromatic hydrocarbons are associated with increased risk of chronic obstructive pulmonary disease during haze events in China. Sci Total Environ. 2017;574:1649–58.
27. Gao N, Wang Y, Zheng CM, Gao YL, Li H, Li Y, et al. beta2-Microglobulin participates in development of lung emphysema by inducing lung epithelial cell senescence. Am J Physiol Lung Cell Mol Physiol. 2017;312:L669-77.
28. Hyzdalova M, Prochazkova J, Strapacova S, Svrzkova L, Vacek O, Fedr R, et al. A prolonged exposure of human lung carcinoma epithelial cells to benzo[a]pyrene induces p21-dependent epithelial-to-mesenchymal transition (EMT)-like phenotype. Chemosphere. 2021;263:128126.
29. Chen XY, Feng PH, Han CL, Jheng YT, Wu CD, Chou HC, et al. Alveolar epithelial inter-alpha-trypsin inhibitor heavy chain 4 deficiency associated with senescence-regulated apoptosis by air pollution. Environ Pollut. 2021;278:116863.
30. Tezze C, Romanello V, Desbats MA, Fadini GP, Albiero M, Favaro G, et al. Age-Associated Loss of OPA1 in Muscle Impacts Muscle Mass, Metabolic Homeostasis, Systemic Inflammation, and Epithelial Senescence. Cell Metab. 2017;25:1374–89 e1376.
31. Jurk D, Wilson C, Passos JF, Oakley F, Correia-Melo C, Greaves L, et al. Chronic inflammation induces telomere dysfunction and accelerates ageing in mice. Nat Commun. 2014;2:4172.
32. Cho SJ, Stout-Delgado HW. Aging and Lung Disease. Annu Rev Physiol. 2020;82:433–59.
33. Sarkar D, Fisher PB. Molecular mechanisms of aging-associated inflammation. Cancer Lett. 2006;236:13–23.
34. Kanderova V, Svobodova T, Borna S, Fejtkova M, Martinu V, Paderova J, et al. Early-onset pulmonary and cutaneous vasculitis driven by constitutively active SRC-family kinase HCK. J Allergy Clin Immunol. 2021; S0091-6749:01395–6.
35. Finney LJ, Belchamber KBR, Fenwick PS, Kemp SV, Edwards MR, Mallia P, et al. Human Rhinovirus Impairs the Innate Immune Response to Bacteria in Alveolar Macrophages in Chronic Obstructive Pulmonary Disease. Am J Respir Crit Care Med. 2019;199:1496–507.
36. Li Q, Verma IM. NF-kappaB regulation in the immune system. Nat Rev Immunol. 2002;2:725–34.

37. Zhang Q, Lenardo MJ, Baltimore D. 30 Years of NF-kappaB: A Blossoming of Relevance to Human Pathobiology. Cell. 2017;168:37–57.
38. Hayden MS, Ghosh S. NF-kappaB in immunobiology. Cell Res. 2011;21:223–44.
39. Zhao H, Wu L, Yan G, Chen Y, Zhou M, Wu Y, et al. Inflammation and tumor progression: signaling pathways and targeted intervention. Signal Transduct Target Ther. 2021;6:263.
40. Bai J, Cervantes C, Liu J, He S, Zhou H, Zhang B, et al. DsbA-L prevents obesity-induced inflammation and insulin resistance by suppressing the mtDNA release-activated cGAS-cGAMP-STING pathway. Proc Natl Acad Sci U S A. 2017;114:12196–201.
41. Yu CH, Davidson S, Harapas CR, Hilton JB, Mlodzianoski MJ, Laohamonthonkul P, et al. TDP-43 Triggers Mitochondrial DNA Release via mPTP to Activate cGAS/STING in ALS. Cell. 2020;183:636–49 e618.
42. Rayman MP. Selenium and human health. Lancet. 2012;379:1256–68.
43. He S, Sharpless NE. Senescence in Health and Disease. Cell. 2017;169:1000–11.
44. Jobeili L, Rousselle P, Beal D, Blouin E, Roussel AM, Damour O, et al. Selenium preserves keratinocyte stemness and delays senescence by maintaining epidermal adhesion. Aging (Albany NY). 2017;9:2302–15.
45. Lee MY, Leonardi A, Begley TJ, Melendez JA. Loss of epitranscriptomic control of selenocysteine utilization engages senescence and mitochondrial reprogramming. Redox Biol. 2020;28:101375.
46. Hammad G, Legrain Y, Touat-Hamici Z, Duhieu S, Cornu D, Bulteau AL, et al. Interplay between Selenium Levels and Replicative Senescence in WI-38 Human Fibroblasts: A Proteomic Approach. Antioxidants (Basel). 2018;7:19.

Figures

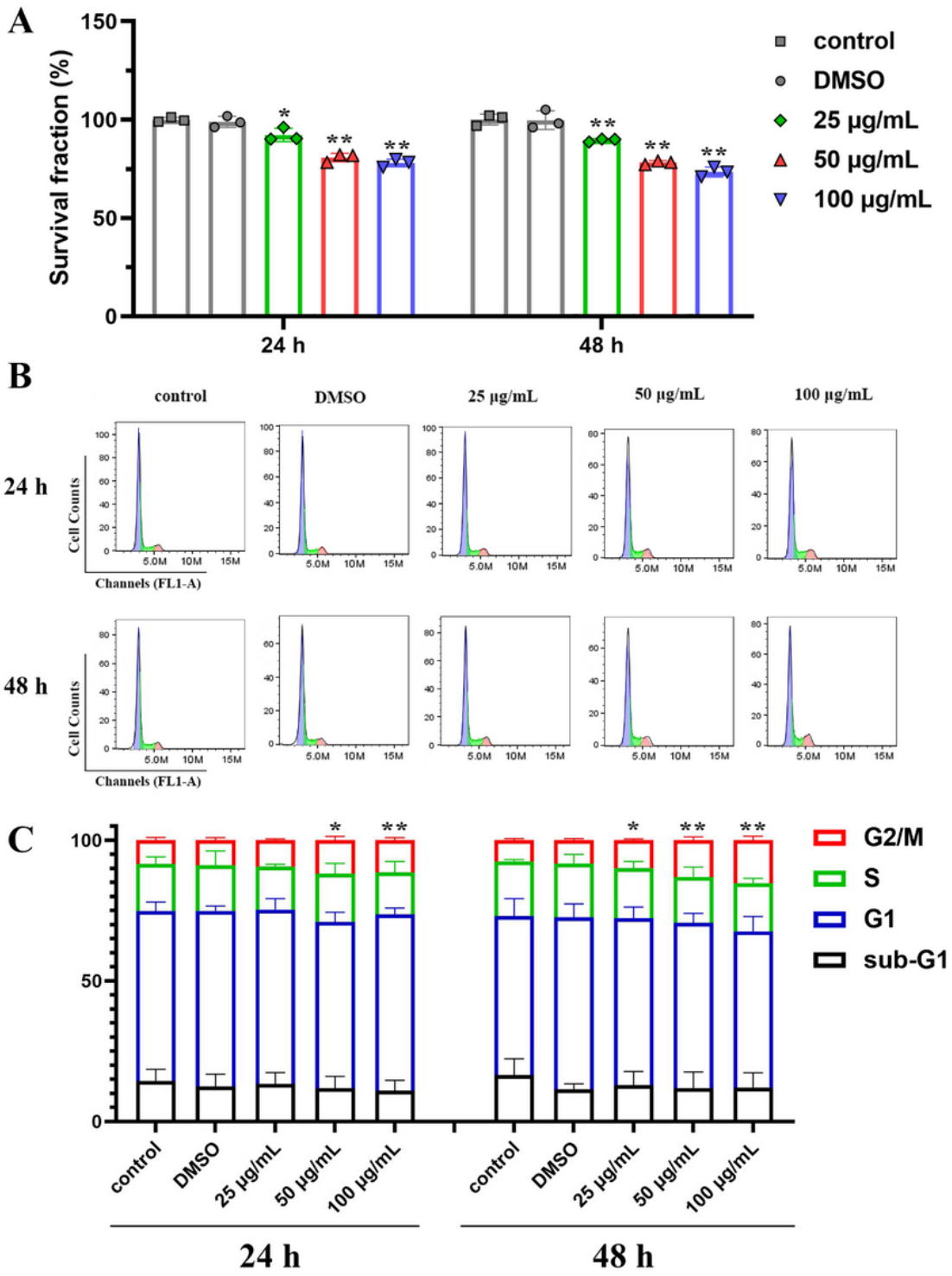

Figure 1

The viability and cell cycle of A549 cells exposed to PM2.5 for 24 and 48 h. (A) The survival fraction of A549 cells. (B) The histogram of cell cycle. (C) The distribution of sub-G1, G1, S and G2/M phase. Data were pooled from at least three independent experiments and represented as mean ± S.D. The symbol (*) and (**) indicated $p < 0.05$ and $p < 0.01$, respectively.

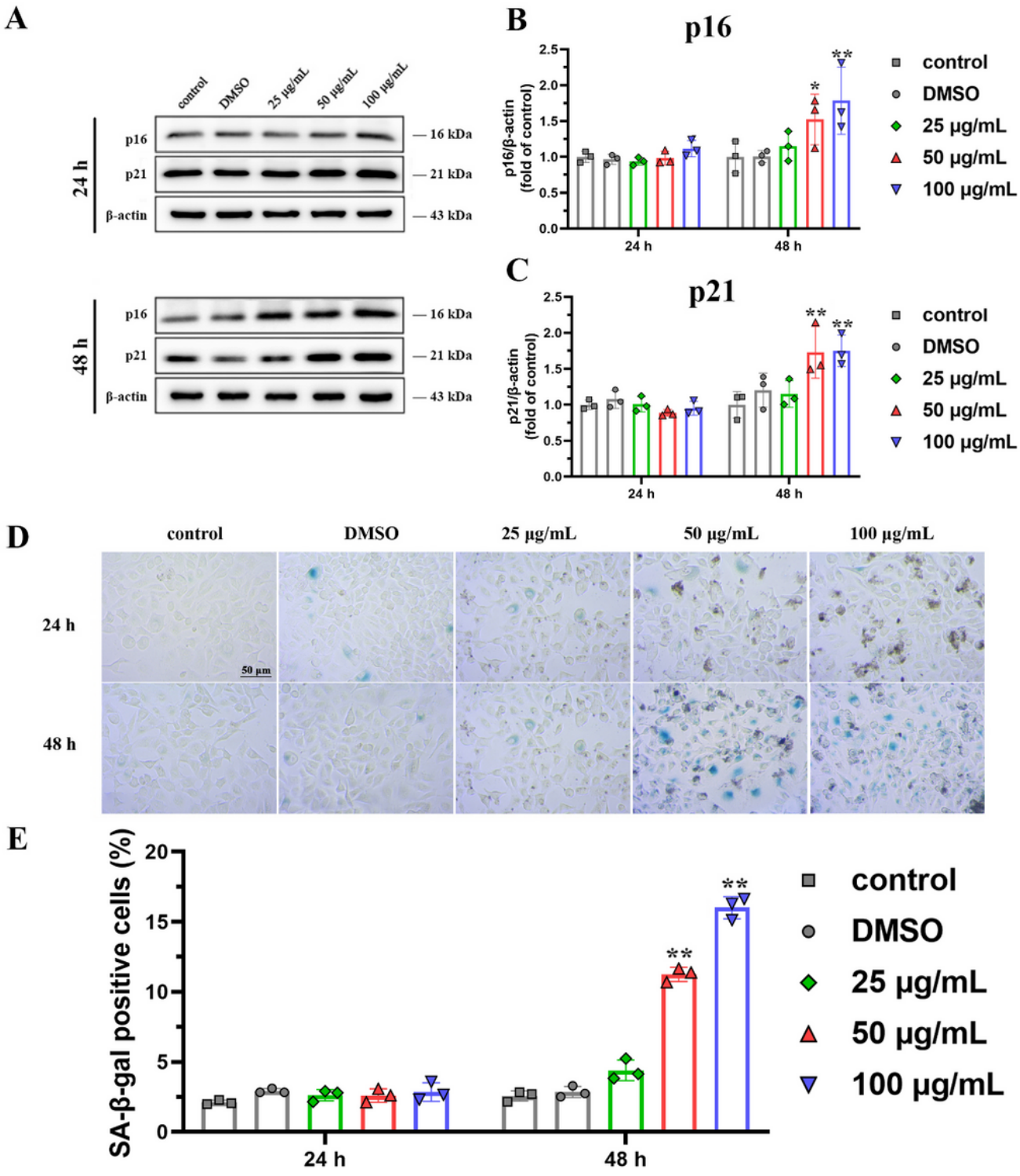

Figure 2

The senescence of A549 cells exposed to PM2.5 for 24 and 48 h. (A) Western blot of p16 and p21 proteins. (B) The expression level of p16 protein. (C) The expression level of p21 protein. (D) Optical images of SA-β-gal foci. (E) The percentage of SA-β-gal-positive cells. Data were pooled from at least three independent experiments and represented as mean ± S.D. The symbol (*) and (**) indicated $p < 0.05$ and $p < 0.01$, respectively.

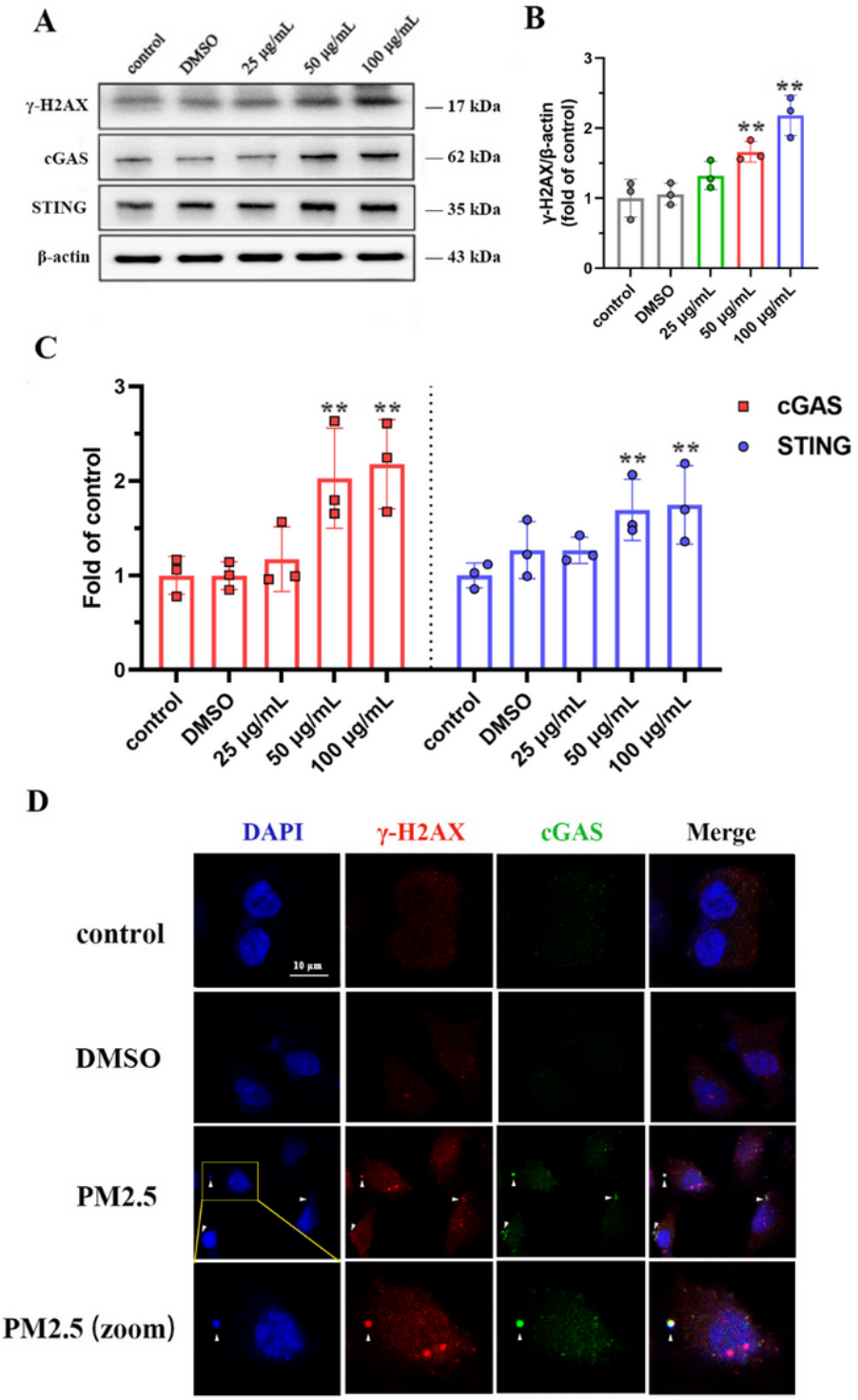

Figure 3

The cGAS/STING pathway in response to DNA damage in A549 cells exposed to PM2.5 for 48 h. (A) Western blot of γ-H2AX, cGAS and STING proteins. (B) The expression level of γ-H2AX protein. (C) The expression level of cGAS and STING proteins. (D) Fluorescence images of A549 cells stained with DAPI, anti-γ-H2AX antibody and anti-cGAS antibody. Zoomed cells highlight colocalization of cGAS with DAPI

and γ-H2AX in the cytoplasmic DNA foci. Data were pooled from at least three independent experiments and represented as mean ± S.D. The symbol (**) indicated $p < 0.01$.

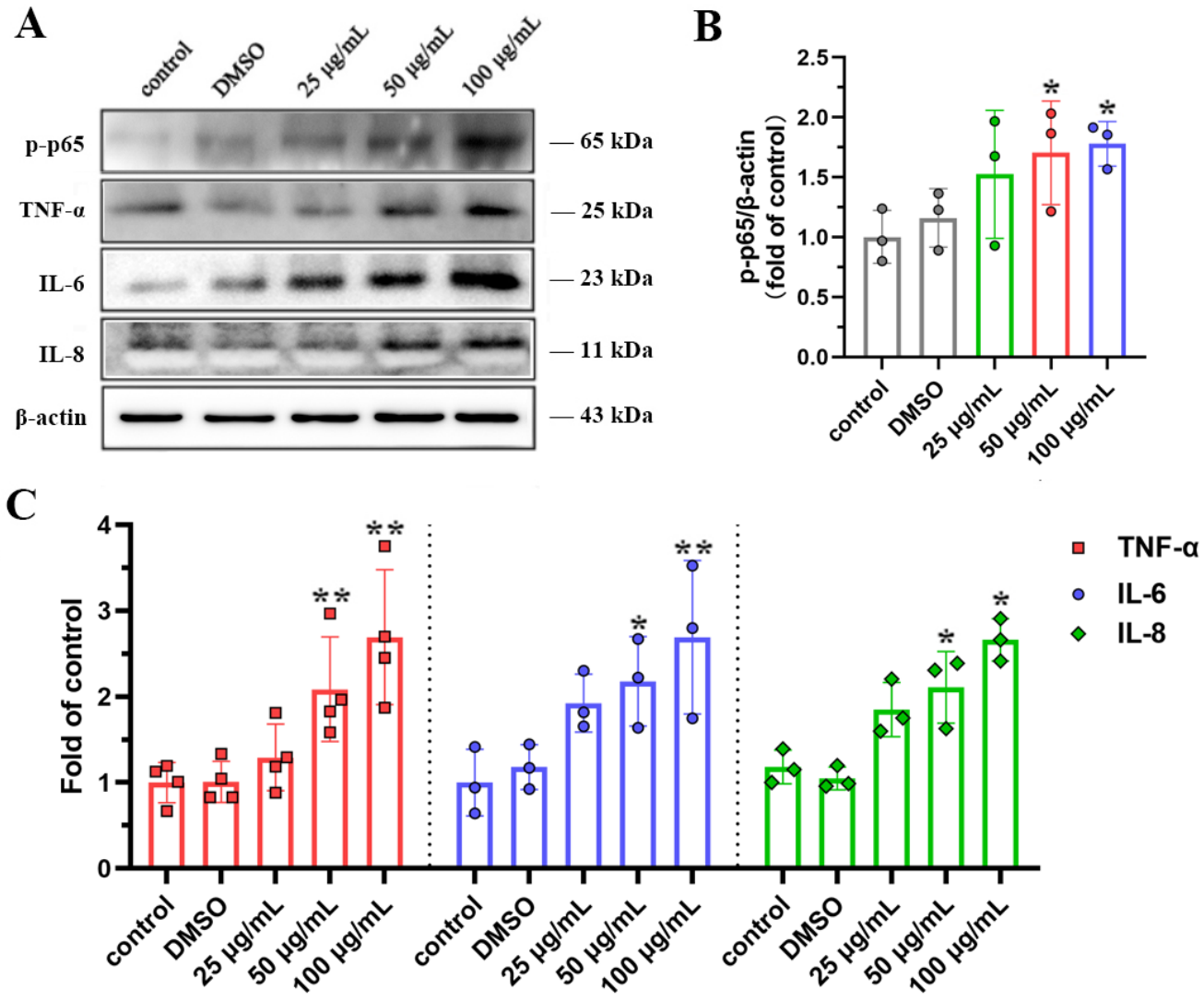

Figure 4

The inflammatory response in A549 cells exposed to PM2.5 for 48 h. (A) Western blot of p-p65, TNF-α, IL-6 and IL-8 proteins. (B) The expression level of p-p65 protein. (C) The expression level of TNF-α, IL-6 and IL-8 proteins. Data were pooled from at least three independent experiments and represented as mean ± S.D. The symbol (*) and (**) indicated $p < 0.05$ and $p < 0.01$, respectively.

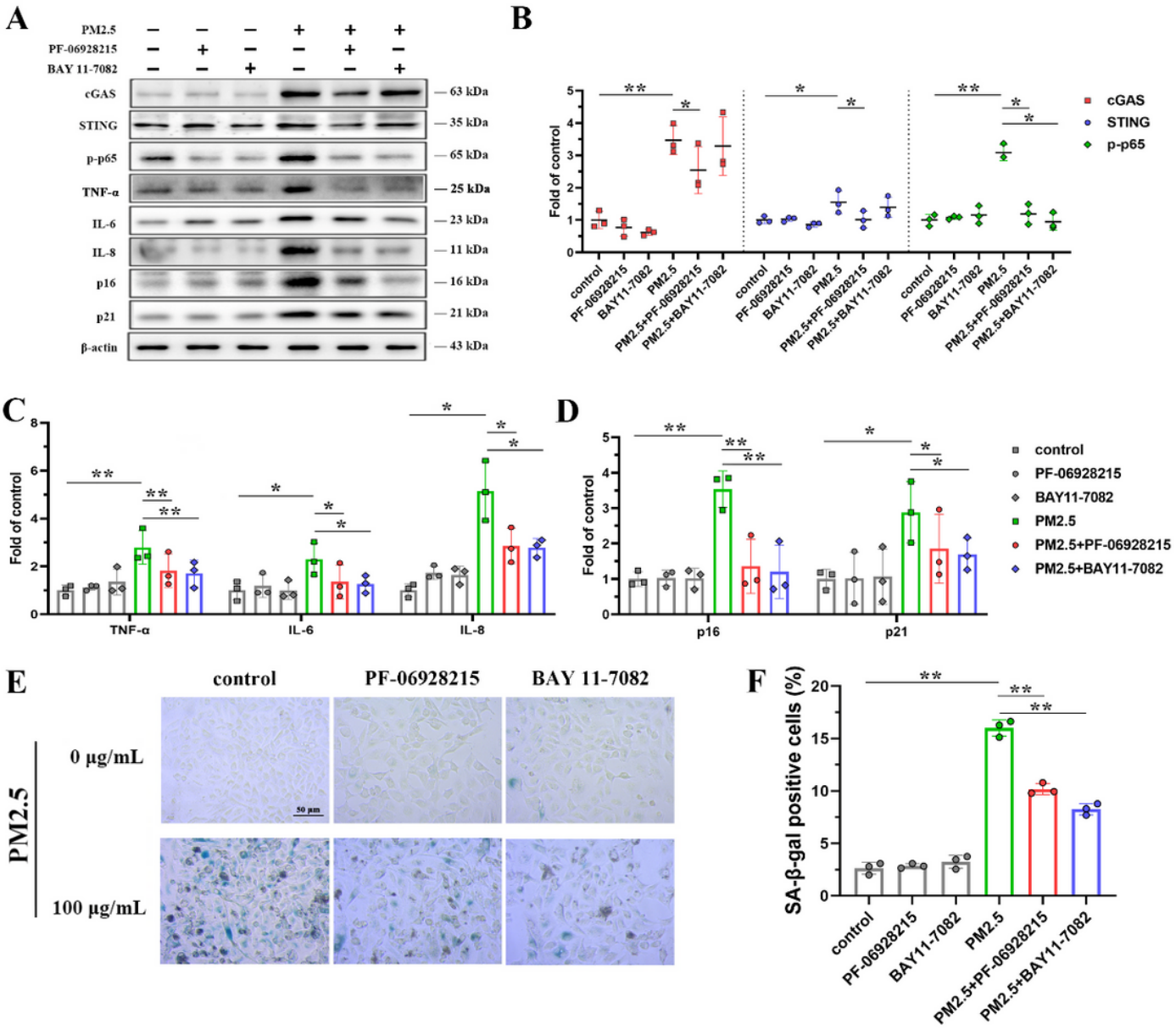

Figure 5

The role of cGAS/STING/NF-κB pathway in regulating cellular senescence in A549 cells exposed to 100 μg/mL PM2.5 with or without 10 μM PF-06928215 and 5 μM BAY 11-7082 for 48 h. (A) Western blot of cGAS/STING/NF-κB pathway- and senescence-related proteins. (B) The expression level of cGAS, STING and p-p65 proteins. (C) The expression level of TNF-α, IL-6 and IL-8 proteins. (D) The expression level of p16 and p21 proteins. (E) Optical images of SA-β-gal foci. (F) The percentage of SA-β-gal-positive cells. Data were pooled from at least three independent experiments and represented as mean ± S.D. The symbol (*) and (**) indicated $p < 0.05$ and $p < 0.01$, respectively.

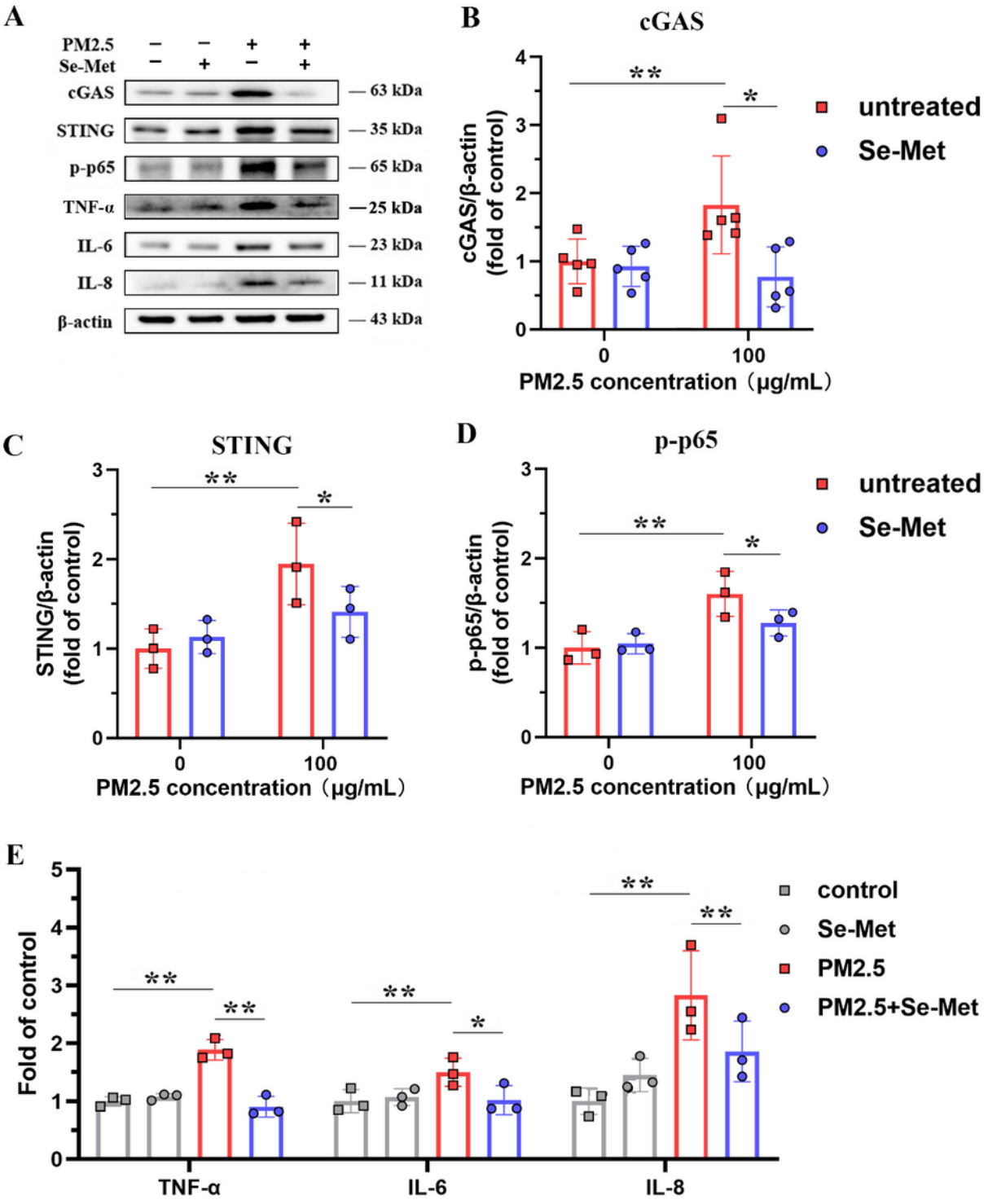

Figure 6

The inhibition of 20 μM Se-Met on the activation of cGAS/STING/NF-κB pathway and inflammatory response in A549 cells exposed to 100 μg/mL PM2.5 for 48 h. (A) Western blot of cGAS/STING/NF-κB pathway-related proteins. (B) The expression level of cGAS protein. (C) The expression level of STING protein. (D) The expression level of p-p65 protein. (E) The expression level of TNF-α, IL-6 and IL-8 proteins.

Data were pooled from at least three independent experiments and represented as mean ± S.D. The symbol (*) and (**) indicated $p < 0.05$ and $p < 0.01$, respectively.

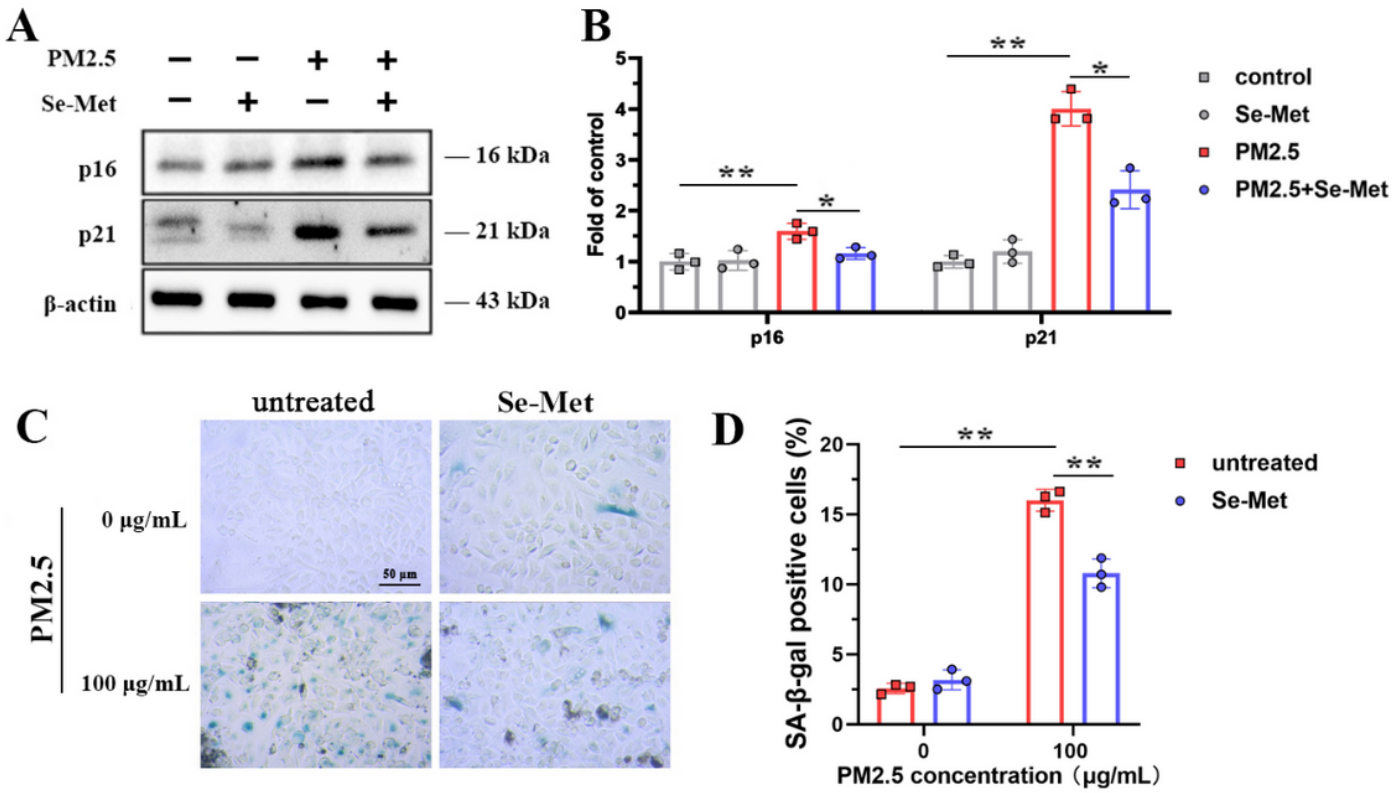

Figure 7

The protection of 20 μM Se-Met on cellular senescence in A549 cells exposed to 100 μg/mL PM2.5 for 48 h. (A) Western blot of p16 and p21 proteins. (B) The expression level of p16 and p21 proteins. (C) Optical images of SA-β-gal foci. (D) The percentage of SA-β-gal-positive cells. Data were pooled from at least three independent experiments and represented as mean ± S.D. The symbol (*) and (**) indicated $p < 0.05$ and $p < 0.01$, respectively.

Supplementary Files

This is a list of supplementary files associated with this preprint. Click to download.

- FigureS1.docx
- FigureS2.docx
- FigureS3.docx
- GraphicalAbstract.docx